DOI:10.1190/segam2020-3427184.1

3D joint inversion of potential field data in the presence of remanent magnetization

Michael Jorgensen and Michael S. Zhdanov, Consortium for Electromagnetic Modeling and Inversion, University of Utah and TechnoImaging*

Summary

In this paper, we develop a method of jointly inverting airborne gravity gradiometry (AGG) and total magnetic intensity (TMI) data in the presence of remanent magnetization. The goal is to obtain structurally similar 3D density and magnetization models. In addition, in the areas with remanent magnetization, one should invert not for magnetic susceptibility, but for a 3D distribution of magnetization vector. This comes at the cost of increased non-uniqueness, which we remedy with joint inversion based on both Gramian constraints or by using joint focusing stabilizers. The Gramian structural constraints are enforced through a correlation of the model gradients. The joint focusing stabilizers are implemented using minimum support approach. We apply this novel joint inversion method to interpretation of the airborne data collected over the Thunderbird V-Ti-Fe deposit in Ontario, Canada. By combining the complementary AGG and TMI data, we generate the jointly inverted models which provide a more consistent image of the geologic structure of the area, simplifying interpretation.

Introduction

Geologic interpretation of 3D physical property models inverted from potential field data for mineral exploration can be complicated by the presence of remanent magnetization. Standard practice for accounting for remanent magnetization is to invert magnetic data for magnetization vector, as opposed to magnetic susceptibility; however, this introduces more degrees of freedom into the inversion and increases non-uniqueness. This complication can be overcome by jointly inverting different geophysical data sets. Total magnetic intensity (TMI) data is generally gathered in airborne gravity gradiometry (AGG) surveys, making the pair a natural choice for joint inversion.

We present two approaches to addressing this problem. The first approach is joint inversion with Gramian constraints (Zhdanov et al., 2012; Zhdanov, 2015), enforcing structural correlation of the gradients of different physical property models. The second approach is joint inversion with a joint focusing stabilizer (Molodtsov and Troyan, 2017; Zhdanov and Cuma, 2018), enforcing joint sparsity via a modified minimum support constraint (Zhdanov, 2015). As an illustration of these approaches, we present the results of inverting the AGG and TMI data collected over the Thunderbird V-Ti-Fe deposit in Ontario, Canada. These data were gathered in a project collaboratively operated between the Ontario Geological Survey (OGS) and the Geological Survey of Canada (GSC). The survey was flown with the Fugro Airborne Surveys gravity gradiometer and magnetic system between 2010 and 2011. The inversion workflow consists of filtering the data, then obtaining 3D standalone inverse models to determine optimal parameters for the joint inversions.

We present the density and magnetization vector model profiles of the Thunderbird deposit obtained from standalone, Gramian, and joint focused inversions. Both Gramian and joint focused inversions provide anomalies with sharper boundaries, stronger structural correlations, and with the same level of data misfit as the standalone inversions. The Gramian inversion yields the highest level of structural correlation; however, the joint focused inversion is easier to implement and faster.

Gramian joint inversion

The geophysical inverse problem is given by the operator equations $m^i = \left(A^i\right)^{-1} d^i$, $(i = 1,2)$, where m^i are the models, A^i are the forward modelling operators, d^i are the data, and the superscript $i = 1,2$ indicates the gravity and magnetic problems, respectively. The solutions of these inverse problems are usually poorly conditioned, so we apply the regularization and minimize a parametric functional using the conjugate gradient method (Zhdanov 2009; 2015).

Separate misfit and stabilizing terms, corresponding to the AGG and TMI data, are combined in the joint parametric functional and subject to the Gramian constraint:

$$P = \sum_{i=1}^{2} \varphi\left(m^i\right) + \alpha \sum_{i=1}^{2} s\left(m^i\right) + \beta G\left(\nabla m^i\right).$$

The misfit terms are defined as follows,

$$\varphi\left(m^i\right) = \left\| W_{d,j}^i \left(A^i\left(m^i\right) - d^i\right)\right\|_2^2,$$

where $W_{d,j}^i$ are the data weights, $A^i\left(m^i\right)$ are the predicted data, and d^i are the observed data. The stabilizing terms are defined as follows,

$$s\left(m^i\right) = \left\| W_{m,j}^i \left(m^i - m_{apr}^i\right)\right\|_2^2,$$

10.1190/segam2020-3427184.1

where $W_{m,j}^i$ are the model weights and m_{apr}^i are the a priori models. The Gramian term is defined by the following formula,

$$G(\nabla m^i) = \begin{vmatrix} (\nabla m^1, \nabla m^1) & (\nabla m^1, \nabla m^2) \\ (\nabla m^2, \nabla m^1) & (\nabla m^2, \nabla m^2) \end{vmatrix},$$

where ∇m^i are the gradients of the models, and $(*,*)$ denotes the inner product (Zhdanov, 2015). As this determinant is minimized, the model gradients are aligned enforcing structural similarity. The process is similar to the cross-gradients approach (Gallardo and Meju, 2003); however, the Gramian constraint allows an exact analytical formula for the gradient direction of the parametric functional, without any approximation typical for the cross-gradients approach, which ensures rapid convergence.

Joint focusing inversion

Separate misfit terms, corresponding to the AGG and TMI data, are combined in the joint parametric functional and subject to the joint minimum support constraint:

$$P = \sum_{i=1}^{2} \varphi(m^i) + \alpha s_{jf}(m^i).$$

The misfit terms are defined the same as above. The joint focusing term is defined as follows,

$$s_{jf}(m^i) = \iiint_V \frac{\sum_{i=1}^{2} W_{m,j}^i (m^i - m_{apr}^i)^2}{\sum_{i=1}^{2} W_{m,j}^i (m^i - m_{apr}^i)^2 + e^2} dv,$$

where e is the focusing epsilon and the index i of the numerator does not equal that of the denominator. Based on standalone magnetization vector inversion results, the vertical component of magnetization vector is dominant in this domain, thus the focusing term incorporates only the density and the vertical component of magnetization vector to reduce non-uniqueness.

To avoid the introduction of spurious features in the joint focusing inversion, the joint minimum support constraint is not enforced until the data misfit corresponding to both models reaches the level $\chi^2 = 2$. This is done by setting the denominator of the joint minimum support constraint $s_{jf}(m^i)$ to unity, which yields a minimum norm stabilizer.

Potential field data is sensitive to the choice of focusing epsilon e. Optimal e for these data was experimentally determined to be 0.95. Smaller values tended to significantly over-focus the models.

Data and model weighting

To ensure stable convergence and minimize inversion artefacts, data and model parameters require additional scaling in the joint inversions.

Both AGG and TMI data are weighted by a function of the errors:

$$W_d^i = \frac{1}{(e_f^i d^i + e_{abs}^i)},$$

where e_f^i are the fractional errors (0.05 for the AGG and TMI data), and e_{abs}^i are the absolute error floors (2-4 Eotvos for the AGG data and 100 nT for the TMI data). Data weights are then further scaled in the joint inversion such that the first misfit for each term $\varphi(m^i)$ is equal to 1:

$$W_{d,j}^i = \frac{W_d^i}{\varphi_{ini}(m^i)},$$

where $\varphi_{ini}(m^i)$ are the initial misfits.

Model weights are determined by the following function of integrated sensitivity:

$$W_m^i = diag\sqrt[4]{F^{i*}F^i},$$

where F^i is the Fréchet derivative of $A^i(m^i)$, and F^{i*} is the complex conjugate. Model weights are then further scaled in the joint inversion by normalizing by the maximum value of the model parameters obtained from standalone inversions:

$$W_{m,j}^i = \frac{W_m^i}{(m_{sep}^i - m_b^i)},$$

where m_{sep}^i are the models obtained from standalone inversions and m_b^i are the background model values.

The regularization terms α, β are adaptively reduced to ensure stable convergence (Zhdanov, 2009; 2015). The inversion is halted when the χ^2 fit corresponding to both misfit terms drops to 1, meaning the interpreted noise level has been reached.

Results

We inverted the data collected over the Thunderbird deposit shown in Figure 1. Based on potential field data and limited core drilling, Thunderbird is assumed to be a semi-massive V-Ti enriched magnetite with a rough volume of 0.32 km3.

DOI:10.1190/segam2020-3427184.1

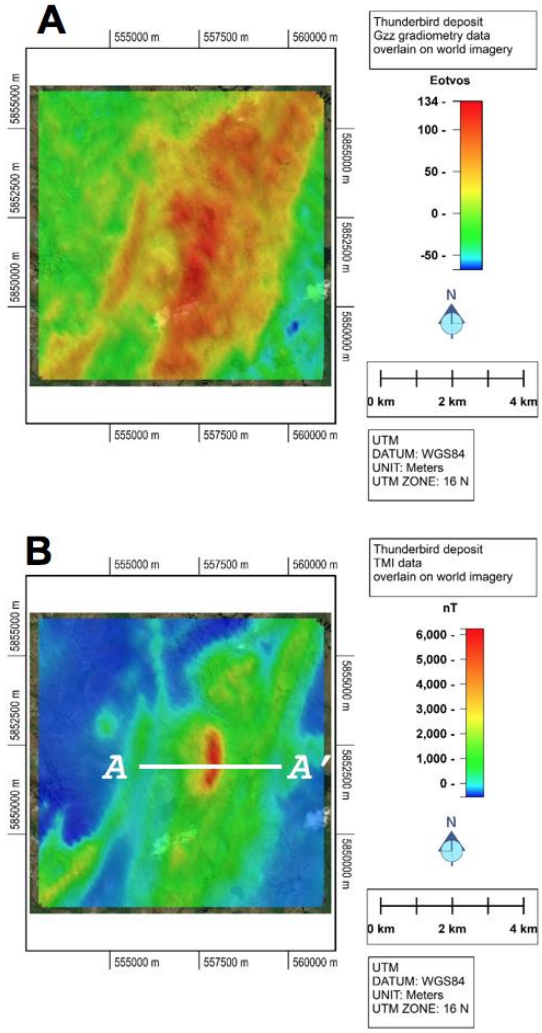

Figure 1: Panel (A) shows the Gzz component of the observed AGG data shown in UTM coordinates. Panel (B) shows the observed TMI data map. The location of profile AA' is shown in white.

TMI data were filtered to eliminate responses from the deeper sources. We inverted the data on a 50x50 m2 horizontal grid with a logarithmic depth discretization ranging from 25-150 m. Total grid size was ~250,000 cells. The inversions were run on a 16-core Intel Xeon desktop with 128 GB memory. Total runtime was ~10 minutes for the standalone AGG inversion, ~5 minutes for the standalone TMI inversion, ~45 minutes for the Gramian joint inversion, and ~15 minutes for the joint focused inversion.

Figure 2 shows, as an example, a comparison between the observed and predicted Gzz component of the gravity gradient field and TMI data produced by standalone and joint inversions. One can see an excellent fit of the observed data by the data computed for the inverse models.

In Figure 3, we contrast the standalone inverted models with the jointly inverted models, which have sharper boundaries and more structural correlation, while maintaining the same level of data misfit as the standalone inversions. The inducing magnetic field direction is shown in Panels 2B, 2D, and 2F, for reference with the inverted magnetization vectors.

It can be challenging to resolve both a geologically meaningful magnetic susceptibility model and a good data fit underlying such a narrow, high-contrast (~1000+ nT) anomaly as that in Panel 1B (Zhdanov and Cuma, 2018). Considering the magnetization vector introduces more degrees of freedom in the inversion; however, that also increases the potential for non-uniqueness, which we remedy with joint inversion.

Conclusions

We have introduced methods of joint inversion of AGG and TMI data in the presence of remanent magnetization using both Gramian and joint focusing constraints. We have jointly inverted AGG and TMI data acquired over the Thunderbird V-Ti-Fe deposit. Comparison of the standalone inverted density and magnetic vector models versus the joint inverted models, which all have the same level of data misfit ($\chi^2 = 1$), demonstrates that the jointly inverted models can recover the more compact bodies, more structural correlation, and more geologically reasonable models than the standalone inverse solutions. The Gramian inversion does provide the highest level of structural correlation; however, the joint focusing inversion is faster computationally.

Acknowledgements

The authors acknowledge Consortium for Electromagnetic Modeling and Inversion (CEMI) at the University of Utah and TechnoImaging for the support of this research. The AGG and TMI data were collected by Fugro and made available by the Ontario Geological Survey, Canada.

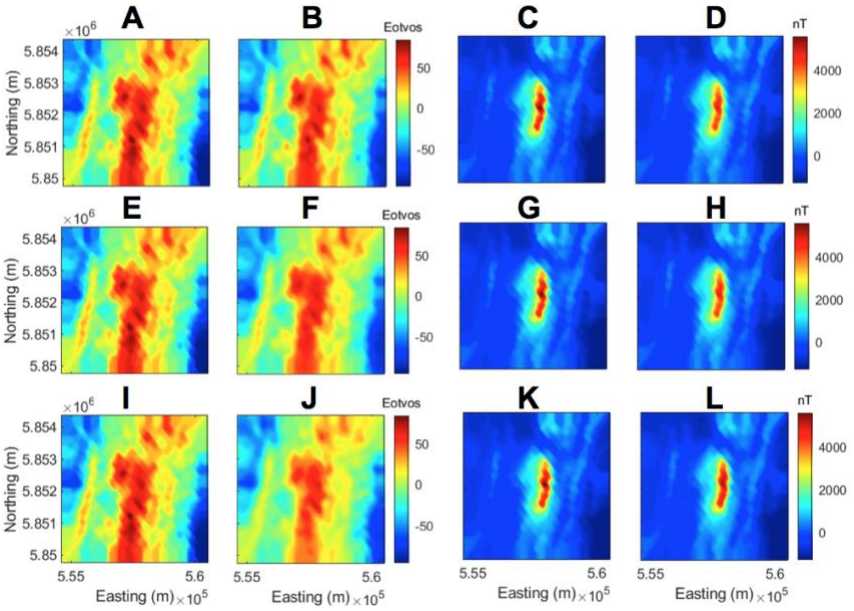

Figure 2: Panels (A) & (B) show observed and predicted Gzz component of gravity gradient field data from standalone inversion, respectively. Panels (C) & (D) show observed and predicted TMI data from standalone inversion, respectively. Panels (E) & (F) show observed and predicted Gzz component of gravity gradient field data from Gramian inversion, respectively. Panels (G) & (H) show observed and predicted TMI data from Gramian inversion, respectively. Panels (I) & (J) show observed and predicted Gzz component of gravity gradient field data from joint focused inversion, respectively. Panels (K) & (L) show observed and predicted TMI data from joint focused inversion, respectively.

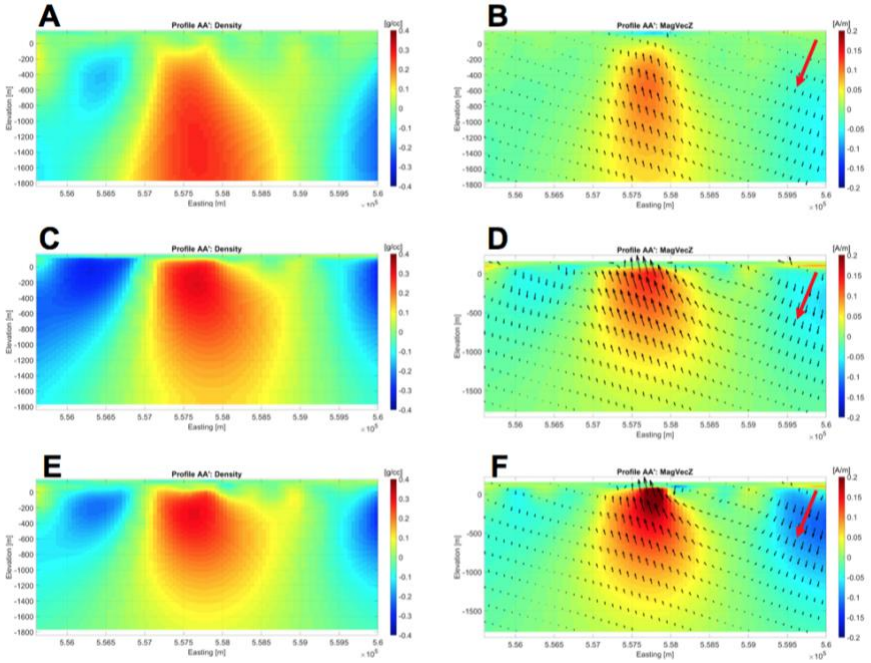

Figure 3: Panels (A) & (B) show vertical sections of the standalone inverted density and magnetic vector models, respectively. Panels (C) & (D) show vertical sections of the Gramian jointly inverted density and magnetic vector models, respectively. Panels (E) & (F) show vertical sections of the jointly focused inverted density and magnetic vector models, respectively. The color map in panels (B), (D), and (F) is the vertical component of magnetic vector, the black arrows are the full magnetic vector, and the red arrows in the upper right corner indicates the direction of the inducing field.

REFERENCES

Gallardo, L. A., and M. A. Meju, 2003, Characterization of heterogeneous near-surface materials by joint 2D inversion of DC resistivity and seismic data: Geophysical Research Letters, **30**, 1658, doi: https://doi.org/10.1029/2003GL017370.

Molodtsov, D., and V. Troyan, 2017, Multiphysics joint inversion through joint sparsity regularization: 87th Annual International Meeting, SEG, Expanded Abstracts, 1262–1267, doi: https://doi.org/10.1190/segam2017-17792589.1.

Zhdanov, M. S., 2009, Geophysical electromagnetic theory and methods: Elsevier.

Zhdanov, M. S., 2015, Inverse theory and applications in geophysics: Elsevier.

Zhdanov, M. S., and M. Cuma, 2018, Joint inversion of multimodal data using focusing stabilizers and Gramian constraints: 88th Annual International Meeting, SEG, Expanded Abstracts, 1430–1434, doi: https://doi.org/10.1190/segam2018-2998495.1.

Zhdanov, M. S., A. V. Gribenko, and G. Wilson, 2012, Generalized joint inversion of multimodal geophysical data using Gramian constraints: Geophysical Research Letters, **39**, doi: https://doi.org/10.1029/2012GL051233.